Infrared Physics & Technology 131 (2023) 104657

Contents lists available at ScienceDirect

Infrared Physics and Technology

journal homepage: www.elsevier.com/locate/infrared

Study of parameters influence on the measurement of vacuum level in parabolic trough collectors' receivers using infrared thermography

María Elena Carra [a,*], Eneko Setién [b], Loreto Valenzuela [a], Rafael López-Martín [a], Carmen Amador [a], Simon Caron [c], Jesús Ballestrín [a], Jesús Fernández-Reche [a], José A. Carballo [a], Antonio Ávila-Marín [a]

[a] CIEMAT-Plataforma Solar de Almería. Ctra. Senes, km 4.5, 04200 Tabernas, Almería, Spain
[b] Tecnalia. Parque Científico y Tecnológico de Gipuzkoa, Mikeletegi Pasealekua, 2, 20009 Donostia-San Sebastián, Gipuzkoa, Spain
[c] German Aerospace Center (DLR), Institute of Solar Research, Plataforma Solar de Almería (PSA), Ctra. de Senes km.5, 04200 Tabernas, Spain

ARTICLE INFO

Keywords:
Infrared Thermography
Source-sensor distance influence on infrared thermography
Solar Energy
Parabolic Through collector

ABSTRACT

The receiver tube of the parabolic trough collectors may suffer a degradation of the vacuum atmosphere between the glass envelope and the absorber tube due to the permeation of gases, mainly hydrogen or air. This is one of the most common issues of heat loss increase in solar fields with this type of solar collectors. The Surface Temperature Method has been used to determine the complete and partial vacuum loss in the annulus of receiver tubes, by measuring the temperature of the glass envelope. In this work, the influences of the meteorological variables and the source distance on the measurement of the temperature by infrared thermography are analysed, as well as the feasibility of using the reflector of the collector itself to measure the sky temperature, parameter necessary to correctly measure the temperature by means of an infrared sensor.

1. Introduction

Parabolic trough collector technology consists of a parabolic reflector, equipped with a drive unit and a solar tracking system that concentrates solar radiation onto a linear receiver tube located at the focus of the parabola. The fluid circulating inside the receiver tube is heated, transforming the solar radiation into thermal energy. The optical concentration of the solar radiation allows the absorber tube to be smaller than the aperture area of the collector. This fact reduces the heat loss because they are a function of the temperature and surface area of the absorber tube.

The receiver is one of the most important elements of any solar system, influencing to a large extent on its overall performance. In the case of parabolic trough collectors, it typically consists of two concentric tubes, one metallic tube called absorber tube, through which the fluid circulates, and the other made of glass. The absorber tube is usually made of a metal substrate, coated with a spectral selective layer to increase the absorptance and reduce the thermal emissivity, preventing heat loss by thermal radiation. These selective layers degrade in contact with air when they are hot, resulting in convection losses. For this reason, the absorber has to be maintained in a vacuum atmosphere. This is achieved with a glass envelope tube to achieve an evacuated annulus between the two concentric tubes. This glass envelope has a high transmittance in the solar spectrum and a low transmittance in the infrared, allowing solar radiation to pass through to the absorber and minimising radiative losses from the absorber.

Thus, one of the phenomena that most influences the thermal performance of a parabolic trough solar collector field is the loss of vacuum between the glass envelope and the absorber tube due to the entry of gases, mainly hydrogen or air. Hydrogen is generated by the decomposition of hydrocarbons circulating in the absorber tube when the heat transfer fluid is the typical thermal oil used in power plants, biphenyl/diphenyl oxide (BP/DPO) is at a temperature above 400 °C, diffusing hydrogen through the absorber wall to the evacuated annulus. On the other hand, air can be introduced into the annulus from the atmosphere. In a commercial parabolic troughs power plant, the composition of the gas responsible for the vacuum degradation was analysed and it was concluded that the predominant gas was air, due to penetration through small cracks in the glass envelope [1]. The loss of vacuum in the receiver tubes generates heat losses, so once of the main maintenance task currently demanded in commercial systems consists in identify receiver tubes with the vacuum atmosphere degraded to repair or replace, and this type of solar fields consists of thousands of units.

* Corresponding author.
E-mail address: ecarra@psa.es (M.E. Carra).

https://doi.org/10.1016/j.infrared.2023.104657
Received 6 April 2022; Received in revised form 10 February 2023; Accepted 14 March 2023
Available online 20 March 2023

Nomenclature

Symbols

A	Surface portion (μm)
A_c	Constant resultant from the IR thermometer's relationship between the signal received and the temperature (μm)
B	Constant resultant from the IR thermometer's relationship between the signal received and the temperature (μmK)
C	Constant resultant from the IR thermometer's relationship between the signal received and the temperature (dimensionless)
c_2	Physical constant of value 14387.752 μmK
H	Distance (cm)
I	Irradiance (W m^{-2})
l	Horizontal distance (cm)
P	Atmospheric pressure (mbar)
q	Radiance (W m^{-2})
RH	Relative Humidity (%)
S	Signal response value of the Sakuma-Hattori equation (dimensionless)
t	Exposure time (ms)
T	Temperature (°C)
W	Wind speed m s^{-1}
ε	Emissivity (dimensionless)
λ	Wavelength (nm)
dΩ	Solid angle (°)
ϖ	Angle (°)
θ	Angle (°)
ϕ	Integrated radiant flux in pixel (dimensionless)
τ	Transmittance (dimensionless)

Acronyms

AOI	Area of Interest (pixels)
ASTM	American Society for Testing and Materials
BP/DPO	Biphenyl/diphenyl oxide
CIEMAT	Centro de Investigaciones Energéticas Medioambientales y Tecnológicas
DNI	Direct normal irradiance (W m^{-2})
FOV	Field of view
HTF	Heat Transfer Fluid
IR	Infrared
PSA	Plataforma Solar de Almería
PTC	Parabolic-trough collector
SCADA	Supervisory control and data acquisition system
SSE	Source Size Effect

Several methodologies have been developed to identify the heat losses in the receiver of a parabolic-trough collector, the stationary method, the quasi-stationary method, the transient method and the Surface Temperature Method. Each method can be apply to operating plants with concentrated solar power, understanding operation condition as the situation where the solar reflector are focused to the sun and concentrating the solar power in the central receptor (lineal and punctual focus). The stationary method is based on the premise that the heat loss power is equal to the electrical heating power required to maintain the absorber at a steady-state temperature level. Thus, with the required input power determined at different temperature levels, the characteristic heat loss curve of the tested receiver is obtained [2]. The quasi-stationary method uses energy balances and the temperature of the glass envelop considering quasi-stationary state [3]. In the transient method, a transient excitation is applied to the absorber tube temperature and the glass envelope temperature response is analysed, using infrared pyrometry and an inverse heat transfer model [4]. This method allows separating heat loss transfer mechanisms, i.e. radiation from the absorber coating and convection in the receiver annulus [5]. The Surface Temperature Method is based on the fact that the glass envelope is transparent to the solar radiation spectrum and opaque to far infrared radiation, therefore, heat losses from the absorber tube will be transferred through the glass envelope. Thus, the radiation and convection heat losses from the absorber tube to the environment are directly related to the temperature of the glass envelope because if there are vacuum losses in the annulus between the absorber tube and the glass envelope, the temperature of the glass will rise due to convection and gas conduction heat losses in the annulus atmosphere. This atmosphere and the heat transfer by convection and conduction will depend on the incoming air due to micro-cracks or micro-pores in the metallic bellows or glass-to-metal seals or hydrogen introduced through the wall of the absorber tube from the hydrocarbons in the heat transfer fluid. This means that, for a given inlet gas, it is possible to calculate the partial vacuum pressure by measuring the temperature of the glass and the absorber tube. The glass temperature can be measured with thermographic cameras or pyrometers and the absorber temperature can be considered as the average temperature of the HTF in the absorber tube, relating it to the linear expansion of the metal with the average temperature or by non-contact methods such as thermographic cameras or pyrometers [6].

The Surface Temperature Method has been validated for the determination of total vacuum pressure in the annulus or complete loss of vacuum pressure in the annulus between the glass envelope and the absorber tube of parabolic troughs' receivers [7,8]. This extended methodology has been used at the Plataforma Solar de Almería-CIEMAT to determine partial vacuum losses in tubes that are not completely damaged. This may be essential for predictive maintenance in this type of solar collector fields [9]. For this purpose, the partial vacuum pressure in the annulus of the parabolic trough collector (PTC) receiver tube and the effect on heat losses were determined, considering air as an incoming gas, by means of an experimental campaign to relate the glass envelope temperature measured with an IR camera, with partial vacuum pressures and the consequent heat losses. This experimental campaign was carried out both in the laboratory and outdoor under real operating conditions. The purpose of the laboratory tests is to obtain controlled results of the glass envelope temperature measurement without the effect of meteorological variables and thus determining whether this method can be used to detect losses due to partial vacuum pressures instead of total vacuum loss. On the other hand, the outdoor measurements were intended to obtain a preliminary analysis of whether the Surface Temperature Method can be applied on a real PTC power plant. The results obtained in the laboratory confirmed that the temperature of the glass envelope increases when the vacuum of the annulus is partially or totally lost. Furthermore, it was observed that the temperature increase is significantly higher when the vacuum was completely lost than when there were partial losses. Therefore, it was confirmed that it is possible to deduce whether there are total or partial losses in the annulus from laboratory measurements. The on-field results obtained were in good agreement with the laboratory data, although the measurement errors were increased due to changes in atmospheric conditions, making it more difficult to detect temperatures associated with partial vacuum pressure losses. Therefore, in the present work, the influence of meteorological variables on the on-field infrared thermography measurement for partial vacuum pressure losses in the annulus has been analysed, carrying out a measurement campaign in a real PTC for six months, with different conditions of the meteorological variables, DNI, ambient temperature, relative humidity, wind speed, wind direction and atmospheric pressure. The error in the glass temperature measurement has

also been studied by varying the sensor-source distance, deriving a correction for this phenomenon, with the aim of eliminating variations and errors in the temperature measurement due to height variations. This is of great importance considering that the Surface Temperature Method is to be scaled to a commercial plant, where the tubes are not easily manipulated for testing, so the measurements to detect partial vacuum losses would be made with a drone whose flight is not regular in height over time, and high accuracy of the glass temperature is needed to detect partial vacuum losses.

Finally, in infrared thermography, the sky temperature needs to be considered in order to correct its influence on the measurement. In the measurement campaign, a mirror with a reflectance value close to 1 was used to set the camera reading of this mirror as the sky temperature. Given the complexity of using a mirror characterised in the measurements in a commercial power plant, carried out with a drone, in this work we also study the possibility of obtaining this sky temperature using the mirror facet of the parabolic trough collectors.

2. Materials and methods

2.1. Instrumentation

The camera selected for all tests has been the Optris Pi640 model, with accuracy ± 2%, resolution 0.075 °C, spectral range 7.5–13 μm and angular range or field of view (FOV) (90°x66°). At this way, camera allows monitoring 3 m of tube length at a distance of 1.5 m with a pixel size of 5x4 mm2. The camera has an optical system that focuses the infrared energy onto a detector with thousands of pixels arranged in a grid. Each of these pixels reacts to the infrared energy received, produced by the value of the temperature emitted, and produces an electronic signal. The camera's processor takes the signal from each pixel and performs a mathematical calculation, creating a colour map of the object's surface temperature [10].

The EUROtrough PTC collector [11] used in the outdoor campaign is placed at southeast to the PSA. This collector has a focal length of 1710 mm and a parabolic aperture width of 5760 mm. The facets are of two types: the inner ones, with size 1500 mm × 1700 mm and the outer ones, with size 1640 mm × 1700 mm. The inner ones have the smaller dimension in the direction of the parabola and the larger in the longitudinal direction. The outer ones have the smaller dimension in the direction of the parabola and the larger in the longitudinal direction. The standard commercial receiver tube used in the laboratory campaign has an absorber tube length of 4.06 m and diameter of 70 mm, and a glass envelope tube diameter of about 115 mm.

The mirror used as reference for the Sky temperature consists of a highly reflecting metal deposited on a substrate and protected by a coating. The composition is aluminium and silvered polymer. It has a 94 % of weighted reflectance (reflectance measured in the OPAC laboratory at the PSA-CIEMAT) and a spectral reflectance of the 89.2 % in the range of 300 to 2500 nm (solar spectrum), and only the only reflectance is in wavelength above 2500 nm, being insignificant in the spectral range of the IR camera [12].

The vacuum pressure in the annulus of the receiver tube is measured with two pirani gauges manufactured by Pfeiffer model PKR 251, with pressure range from ($5 \cdot 10^{-9}$ to 1000 mbar). The used thermocouples are type K-class I for the absorber and ambient temperature and type T-class I for the measure.

The electric heating system consists in an aluminium cylinder of 4.06 m of length and 0.055 m of diameter, inside of the absorber tube. This cylinder is heated by eight electrical heaters of 6.3 Ω/m connected to two electrical power supplies. In addition, two extra small electrical heaters of 750 Ω are located in both ends of the cylinder. The electrical supplies are model N8740A manufactured by Agilent Technologies. These electrical power systems can supply a maximum of 3300 W (150 V, 22 A) DC each one.

Direct solar radiation is recorded by a pyrheliometer spectrally flat class A located in the vicinity of the PTC loop and with a spectral range of 200 to 4000 nm. Wind direction is recorded by a normal meteorological anemometer located near the collector at 10 m and 12 m heights, although wind direction is only recorded at 10 m. Relative humidity, ambient temperature and atmospheric pressure are also recorded using normal meteorological instrumentation located at the PSA.

2.2. Experimental measurement campaign

A measurement campaign was carried out in the laboratory to obtain the ratio of the glass envelope temperature measured with an IR camera and the partial vacuum pressure losses and heat losses in a PTC. In this laboratory environment, the aim was to minimise the effect of meteorological parameters on the measurements. On the other hand, another outdoor experimental campaign was carried out in a PTC test loop of the Plataforma Solar de Almería (PSA) with real operating conditions in order to check whether the Surface Temperature Method can be applied in a real PTC power plant. To this end, it has been checked whether the results obtained outdoors coincide with those obtained in the laboratory, detecting how meteorological variables affect the measurement and being able to use corrections in the event that they do affect the Surface Temperature Method in a real plant to obtain the partial vacuum losses and carry out predictive maintenance of this type of collectors.

In the outdoor measurement campaign, the mirror with 94% solar–weighted reflectance was used to set this IR camera measurement as Sky temperature. At the same time, measurements of a mirror area of the parabolic trough collector were recorded to check if both measurements are coincident and with future drone measurements on real power plants, the Sky temperature can be obtained directly from the collector.

On the other hand, a measurement campaign was carried out to obtain the glass temperature errors by varying the glass envelope-infrared camera distance difference. Preliminary measurements were carried out in the PSA receiver tubes laboratory to check that the temperature reading varies with the sensor-source distance, and then an outdoor test was carried out by varying the camera-tube distance in a range from 1 to 5 m, a distance that resembles the drone-tube distance. This is the way how heat losses would be measured in a commercial power plant, as this is the distance at which the drone would fly to perform predictive maintenance measurements in a real plant.

2.2.1. Glass envelope temperature at different partial pressures: Preliminary laboratory tests

Measurements were taken in the laboratory for characterisation of receiver tubes at PSA to detect the vacuum losses in the space formed between the absorber tube and the glass envelope. Glass temperature measurements of the standard commercial receiver tube tested were taken with an infrared camera at different vacuum conditions in the glass-absorber tube space (10^{-4}, 10^{-2}, 10^{0}, 10^{2} and 10^{3} mbar) and at different absorber tube temperatures (100 °C, 200 °C, 300 °C, 350 °C, 400 °C) [9]. The temperatures of the absorber tube were reached using electrical resistances inserted along an aluminium cylinder introduced into the absorber tube. Absorber temperature is monitored with thermocouples distributed along the inside face of the absorber. The cavity between the absorber and the glass envelope is pressurised with a vacuum pump system. A Pirani gauge is used to measure the vacuum pressure in the annulus. The infrared camera used was installed on a mechanical arm in order to measure temperature from different angles. In addition, the temperature of the glass envelope was monitored with thermocouples and stickers of known emissivity that were added to it, in order to facilitate accurate temperature measurements of the glass with the IR camera. The measurements were carried out according to ASTM E2847-14 [13], that is, the surface temperature of the glass is determined by removing the distorting effects of the reflected radiation, atmospheric attenuation and the emissivity of the surface to the camera detector. The effect of the reflected thermal radiation (temperature) is calculated with the reflector method by placing an infrared reflector,

mainly an aluminium mirror, perpendicular to the camera normal and parallel to the surface to be measured. The camera temperature value for the pixels where the reflector is located is measured with emissivity 100% and will be the reflected ambient temperature, including atmospheric absorption. In the case of laboratory measurements, the emissivity of the measured surface is obtained by adjusting the emissivity in the camera settings until the measured temperature coincides with that of a thermocouple located around the position measured by the camera.

2.2.2. Glass temperature at different partial pressures, effect of meteorological variables on measurements and of Sky Temperature: Outdoor tests

In order to be able to apply the Surface Temperature methodology in a real PTC power plant, it is necessary to study that the meteorological variables relative humidity, temperature, wind speed, wind speed direction, atmospheric pressure and DNI, to confirm these variables do not affect the infrared camera measurement of the glass envelope temperature, thus reliably obtaining the partial vacuum losses. For this purpose, a test campaign of outdoor measurements of the glass temperature of a real PTC in one of the pilot plants of the PSA, the EUROtrough PTC collector, was carried out [14].

Measurements were taken with different vacuum pressures in the glass absorber tube annulus (10^{-4}, 10^{-2}, 10^{-1}, 10^{0}, 10^{1}, 10^{2}, 10^{3} mbar) and different absorber tube temperatures (200 °C, 250 °C, 300 °C, 320 °C) to compare them with those obtained in the laboratory, with the purpose to quantify the influence on the measurement of the meteorological variables monitored in outdoor tests. The on-field set-up is similar to the laboratory set-up, i.e. the IR camera was installed 1.5 m from the receiver tube on a mechanical arm, and a high reflectance mirror was installed in the glass surface to obtain the sky temperature (Fig. 1). In addition, the figure shows the thermocouples installed to monitor the temperature of the glass at the same time as it is recorded with the IR camera during the tests.

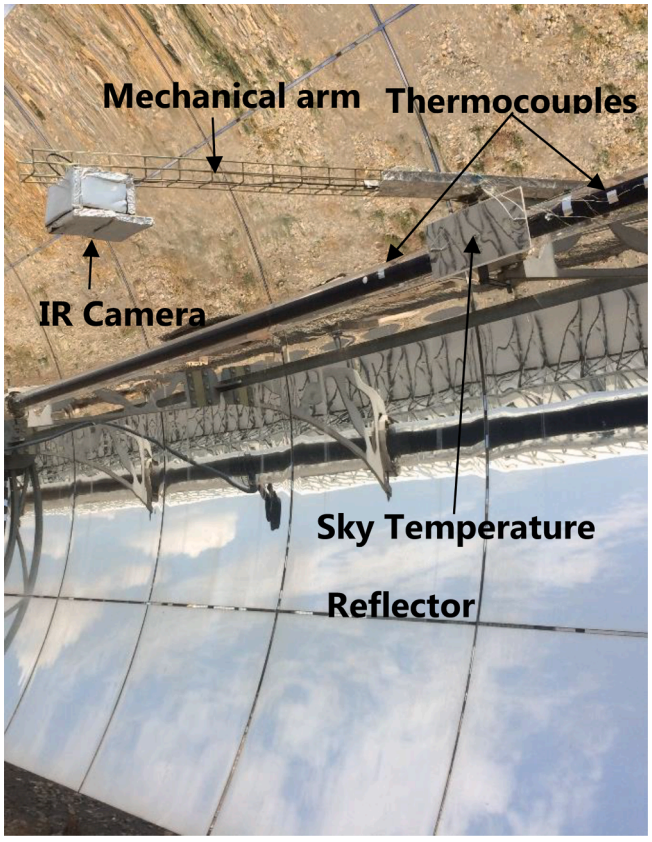

Fig. 1. Outdoor test setup for measuring temperature of PTC receiver tubes with an IR portable camera, receiver tube and mechanical arm to support the IR camera, thermocouples attached to the glass envelope and a reflector installed to measure the Sky temperature.

The temperature of the absorber tube is controlled by the temperature of the heat transfer fluid circulating inside the absorber tube along the PTC, with two thermocouples at the inlet and two thermocouples at the outlet, the tube temperature being considered the average of the four temperature values. DNI, wind direction and speed, relative humidity and ambient temperature are recorded during the test campaign.

To determine whether the PTC mirror itself can be used instead of a reflector, as this would be unfeasible for drone measurements; measurements were made during the campaign of an area of interest (AOI) of the added reflector, as well as an AOI of the mirror area itself to determine the differences in the wind speed and wind speed direction.

The outdoor tests were carried out for approximately 6 months, from June to December 2017, in order to have as much representation as possible of different atmospheric conditions and the consequent variation of the value of these meteorological variables.

2.2.3. Effect of the infrared source-detector distance on the measurement error

In the measurement campaign carried out to study the influence of meteorological variables, it was detected that by varying the distance of the Infrared camera (IR camera) from the parabolic trough collector, the temperature reading of the glass measured varied by a few degrees. As the IR camera moves away from the source, the measured temperature decreases. According to the IR camera measurement procedure, there should be no difference in the temperature reading as the camera detects the maximum wavelength at which the glass envelope emits infrared radiation according to its temperature. With distance, the radiation reaching the camera would be attenuated (less radiation flux), but the maximum wavelength peak would be the same. The IR camera should therefore record the same temperature, even if the camera-source distance varies, although in practice this has been found not to be the case.

This phenomenon can affect the drone measurement of vacuum losses, as the flight during the measurement does not necessarily have to be regular in height, as there may be variations of a few metres or centimetres. To study the influence of the height on the measurement, some measurements were made in the laboratory of tubes to measure the temperature of the glass of a collector at three different heights. These heights are not very different from each other due to the impossibility of measuring several metres high because of the laboratory infrastructure. The experimental setup can be seen in Fig. 2 (a).

Temperature was measured at four different IR camera-tube distances H1 = 118 cm, H2 = 124.5 cm, H3 = 176.5 cm and H4 = 184.5 cm, distances from the floor measured at the vertical support of the IR camera as shown in the figure below Fig. 2 (a). At position H4 the distance between the glass envelope and the IR camera is 70 cm, and at positions H3, H2 and H1 the distances are 62 cm, 10 cm and 3.5 cm respectively. At all these distances, the temperature of the glass envelope was measured at different temperatures of the absorber tube, heated in the range from 25 to 300 °C.

As in this preliminary laboratory test it was observed that there were different glass temperature variations at a distance of only 70 cm, outdoor tests were carried out so as not to have height limitations and to be able to carry out the tests simulating the height that the drones would have when measuring the glass envelopes temperature in a real PTC solar field (approximately 5 m in height). For this purpose, the setup shown in Fig. 2 (b) was prepared. The setup consists of the standard commercial tube used in the laboratory tests, monitored by a SCADA system to control the temperature of the absorber during the tests. The reflectance mirror is installed underneath the tube to use the IR camera measurement in this AOI as Sky Temperature. The glass envelope temperature is monitored with thermocouples and stickers of known emissivity to obtain the IR camera temperature as accurately as possible. The IR camera is mounted on the articulated arm of a lifting platform, which

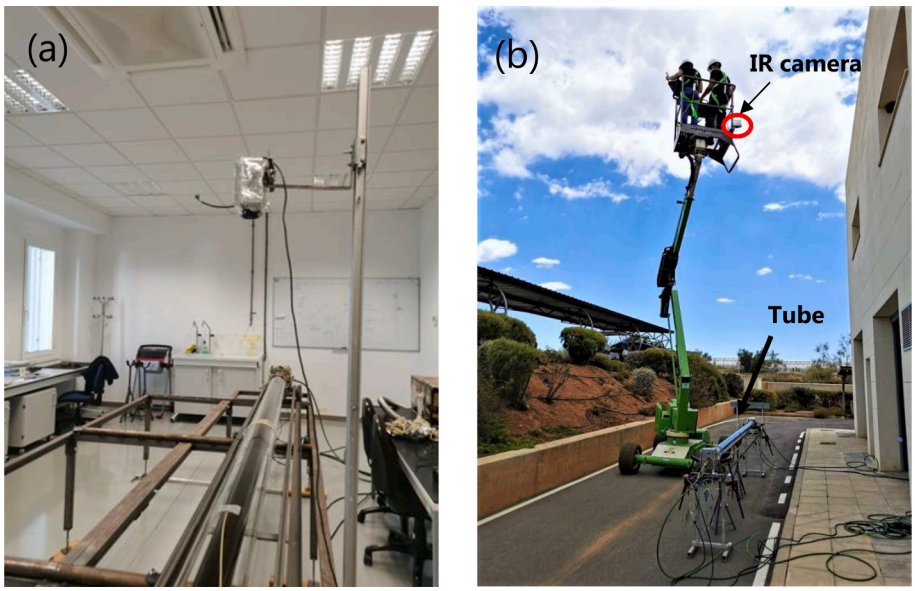

Fig. 2. Experimental device to determine the influence of the camera-source distance on temperature measurement with infrared cameras. Left. Tests in the tube characterisation laboratory of the Plataforma Solar de Almería. Right. Outdoor tests at higher altitudes.

can be adjusted so that the IR camera measuring direction is completely vertical in direction to the absorber tube and the IR camera-tube distance can be easily varied. Measurements were made at distances of 1 m, 2 m, 3 m, 4 m and 5 m distances from absorber tube temperatures of 100 °C, 200 °C, 300 °C and 400 °C. At an ambient temperature of 25 °C it was impossible to carry out the test because, as the receiver-tube was outdoors, solar radiation itself heated the tube to 100 °C.

3. Obtaining the glass envelope temperature with the infrared camera

The glass envelope temperature data measured with the IR camera has been measured according to the standard *ASTM E2758-10 Standard Guide for Selection and Use of Wideband, Low Temperature Infrared Thermometers* [13] whose guidelines state that the temperature of the surface to be measured is determined by removing the distorting effects of the reflected temperature, atmospheric attenuation and the emissivity of the surface from the IR camera detector signal. The reflected temperature is calculated with the reflector method, as mentioned above. In the case of outdoor data, as is also recommended in ASTM E2758, the final glass envelope temperature has been determined using the Sakuma-Hattori equation. The Sakuma-Hattori equation is a mathematical model that calculates the amount of radiation emitted by a perfect black body or received by a thermal radiation detector. This radiation can be thermal radiance, radiometric flux or radiometric power [15]. Eq. (1) shows the Planckian Form of the Sakuma-Hattori equation used, where S is a dimensionless scalar to the amount of radiant flux received by the detector. As input parameters of the calculus we use the temperature given as output by the IR camera, T_{IRT}, the emissivity introduced in the configuration of the camera, ε_{IRT}, the real reflected temperature (Sky temperature) obtained with a high reflectance mirror, T_{surf}, the reflected temperature introduced as parameter in the configuration of the camera when taking the measurement, $T_{REFL\text{-}IRT}$, and the real emissivity of the glass at its corresponding temperature, ε_{SURF}, measured by the thermocouple attached to the glass. This emissivity was obtained in the receiver tube characterisation laboratory by monitoring the tube at different temperatures and obtaining its emissivity [9]. Eq. (2) represents reciprocal form of Sakuma-Hattori equation and the Eq. (3) shows the first derivative of the Sakuma-Hattori equation. In these equations c_2 is a physical constant of value 14387.752 μmK. A_c, B and C are constant resultant from the IR thermometer's relationship between the signal received and the temperature and λ_0 is the IR thermometer's center wavelength based on a simple average of the IR thermometer's high and low spectral range limits. As a result of applying this mathematical model, the real temperature of the glass envelope measured with the IR camera is obtained.

$$S(T) = \frac{C}{exp\left(\frac{c_2}{\lambda_c T+B}\right)-1} \quad (1)$$

$$T = \frac{c_2}{A_c ln\left(\frac{C}{S}+1\right)} - \frac{B}{A_c} \quad (2)$$

$$\frac{\partial S}{\partial T} = [S(T)]^2 \frac{A_c c_2}{C(A_c T+B)^2} exp\left(\frac{c_2}{A_c T+B}\right) \quad (3)$$

$$A_c = \lambda_0\left(1-\frac{\Delta\lambda^2}{2\lambda_0^2}\right) \quad (4)$$

$$B = \frac{c_2 \Delta\lambda^2}{24\lambda_0^2} \quad (5)$$

$$\varepsilon_{SURF} S(T_{SURF}) + (1-\varepsilon_{SURF}) S(T_{REFL}) = \varepsilon_{IRT} S(T_{IRT}) + (1-\varepsilon_{IRT}) S(T_{REFL-IRT}) \quad (6)$$

4. Results and discussion

In this section there will be presented the results and analysis obtained after the laboratory and outdoor tests, where the influence of the meteorological variables observed in the measurement of the glass envelope temperature, the influence of the IR camera-source distance in the measurement and comparison of the Sky temperature obtained through the reflector of the solar collector with the data obtained with a reflector target positioned perpendicularly to the camera during the tests are obtained. In the previous work realised as a preliminary work of this methodology it was done an exhaustive development of the uncertainties [9]. In these calculations it was clear that when the IR camera measurement is done at 0° of the tube, the error of various influent parameters can be obviated. The calculation of the errors has been well developed in the aforementioned document; therefore they have not been reproduced in the present document. For error propagation, the IR camera error (2%) and the relative errors of the meteorological variables have been taken into account.

4.1. Influence of meteorological variables

Fig. 3 shows a first approximation of the differences between the glass temperature measurements made under the same conditions of vacuum partial pressure-glass temperature, in the laboratory and outdoors. The differences found between both values (laboratory-outdoor) differ in some degrees between them, always below 10 °C, except in the case of the total vacuum loss, i.e. when in the annulus there is atmospheric pressure, where these differences are greater than 10 °C. Even so, the differences between the heat losses measured in the laboratory and outdoors are not of a very high order of magnitude. It is also observed that for the same vacuum partial pressure (0.01 mbar i.e.), the temperature recorded by the IR camera is different according to the temperature at which the absorber tube is (200 °C or 300 °C). This indicates that the surface temperature method, when used in a plant with heat transfer fluid through the receiver tube, detects more temperature and, therefore, more thermal losses the higher the temperature of the fluid.

Fig. 4 shows the outdoor glass temperature values measured with the IR camera that have been compared with temperature values measured under similar conditions (laboratory conditions). It is shown too the relative error between both measurements. There are some outdoor tests that could not be compared with the laboratory tests because the vacuum partial pressure during the test does not coincide with the vacuum partial pressure measured in the laboratory at the defined absorber tube temperature or because the absorber temperature does not coincide with the same temperature level recorded in a laboratory test. This is because sometimes the temperature of the HTF in the absorber tube in outdoor installations could not be stabilised at the exact operating temperature intended.

It can be observed, on the one hand, according to the data shown in Fig. 4, that the relative errors of the temperature of the glass envelope measured with the IR camera in the outdoor solar collector are 15 % lower than the glass temperature obtained with the IR camera in the laboratory under the same measurement conditions (temperature of the receiver tube, vacuum partial pressure). Although in most of the tests the error has been in the order of this value, in some tests this difference has been somewhat higher, between 20 and 25 %. The cause of this somewhat higher error may be due to the influence of meteorological variables on the outdoor collector measurements.

The meteorological variables in the laboratory condition were relative humidity 25 %, ambient temperature 25 °C and zero value for wind speed, wind direction and DNI. Laboratory tests were conducted under controlled atmosphere during the entire test period. During the six-month outdoor measurement campaign, data were recorded for ambient temperature, relative humidity, DNI, atmospheric pressure, wind direction and wind speed at different heights (5 m, 10 m and 12 m). Therefore, if the atmospheric conditions affect the measurement, the measurements taken under the same conditions (receiver tube temperature-vacuum partial pressure) during the 6 months of the campaign would be of different values from each other. Fig. 4 shows that in the case of the measurements at 200 °C (absorber tube temperature), the measurements made at a vacuum partial pressure of the order of 10^{-2} mbar present values close to each other, showing a high repeatability of the result. They show differences inferior to 5 °C among them in the most extreme cases, not very significant differences, considering that they may be due to the intrinsic errors of the measurement and the errors of applying the mathematical model of Sakuma-Hattori. In the case of an absorber tube of 300 °C, the differences are on average lower than 5 °C, although there is a difference of 10 °C in the extreme cases. This difference may also be due to the fact that it was observed that in some tests at this temperature level the absorber tube did not always have an exact temperature of 300 °C, but that in some tests the absorber temperature was sometimes up to 20 °C higher due to the impossibility of stabilising the tube temperature at exactly 300 °C during the solar field operation of those days, as noted above.

In order to see if meteorological variables can influence the outdoor measurements and that these do not coincide with those taken under the same conditions of absorber tube temperature and vacuum partial pressure in the laboratory, the measurements have been analysed by sets

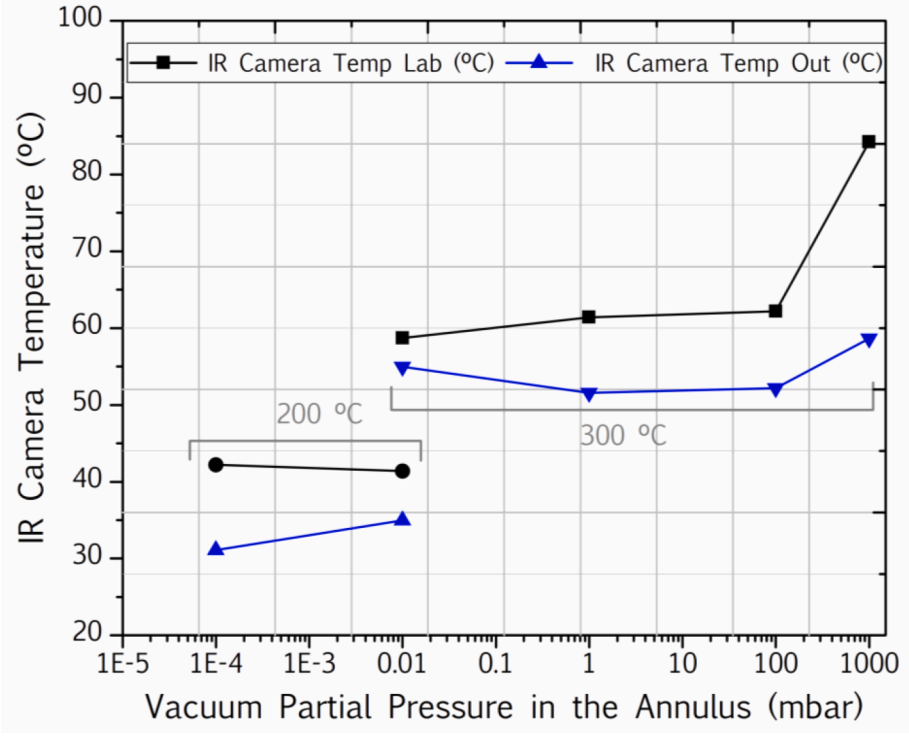

Fig. 3. Temperature measured with the IR camera in tests carried out at different vacuum partial pressures in the annulus (between the absorber tube and the glass envelope) and absorber tube temperatures of 200 and 300 °C in the laboratory and outdoor.

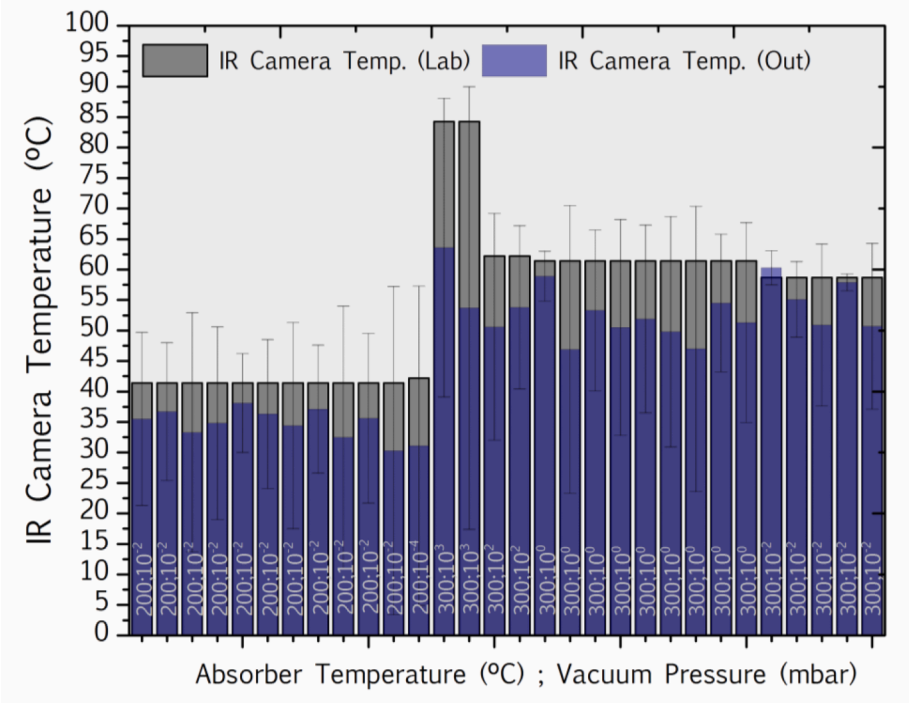

Fig. 4. Temperatures of the glass envelope taken in the laboratory and outdoor with the IR camera and relative error of these measurements. The value for the horizontal axis of each bar means the absorber temperature (200 °C or 300 °C) and the Vacuum Pressure is the second data. Both values are separated in the bars by semicolons.

of tube temperature-vacuum partial pressure conditions as shown in the Fig. 5, where the relative error of the outdoor measurement with respect to the laboratory measurement and the variation of the meteorological variables monitored in the tests has been represented in different graphs for the temperature range from 200 °C and 300 °C. In this way, it can be seen that if the error is higher than the average in a test, its cause may be the influence of the meteorological variables. It has been observed that the relative humidity does not have a great impact on the measurements because the humidity recorded during the campaign were not high, but rather low and stable in all the tests. Therefore, there has been little water vapour in the atmosphere to influence the measurements, so it is certainly not possible to determine if humidity influences the measurement due to the characteristics of this parameter at the PSA site during the trials, usually with a generally low relative humidity (RH) environment for most of the year. Atmospheric pressure (P), DNI and ambient temperature (T) have remained relatively constant in the tests and have not been found to have a major influence on the measurement. It should also be noted that some factors introduced by these variables that may affect the measurement have been considered in the reflected temperature used in the measurement. It has also been seen, especially

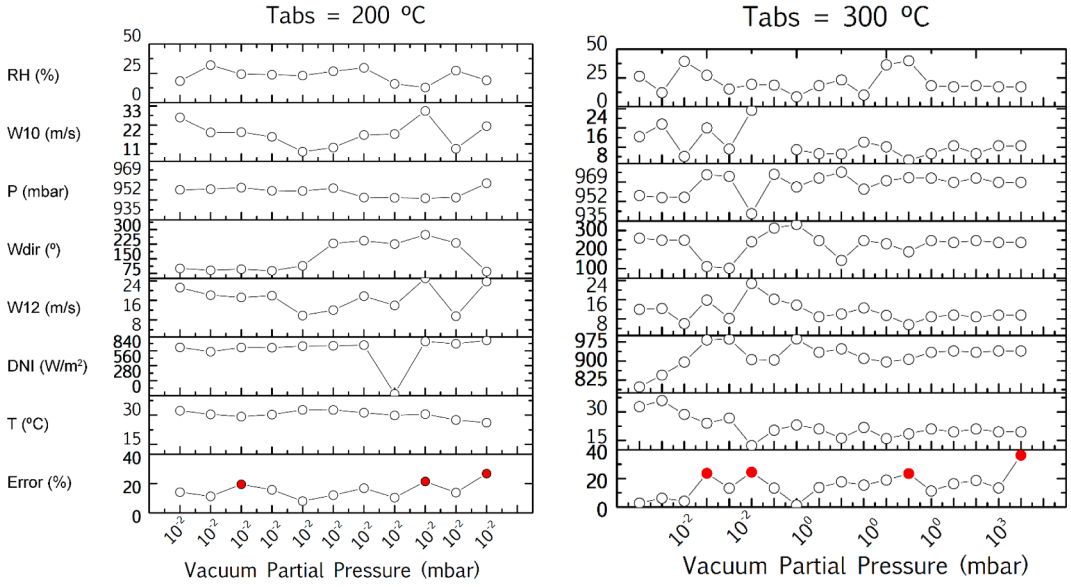

Fig. 5. Error of the outdoor glass envelope temperature measured with the IR camera compared to the measurements obtained in the laboratory and influence of meteorological variables on error. Where RH is the Relative Humidity, W10 is the wind speed at 10 m, W12 is the wind speed at 12 m, P is the atmospheric pressure, Wdir is the wind speed direction, DNI is the Direct Normal Irradiance and T is the ambient temperature.

in the 300 °C tests, that some errors have been higher than average when the DNI is somewhat higher, although this peak of the error value also seems to be correlated to wind speed (W).

Wind speed is the variable with high influence on the measurement error. It is observed that the error curve coincides in trend with the wind speed curve, with the errors being higher at higher values of the variable. Even so, although the wind has an influence on the measurement, increasing the error, it was observed that for outdoor tests with the same absorber tube temperature-vacuum pressure conditions, the values of the glass temperature measured did not differ much from each other, presenting little dispersion, as can be seen in the Fig. 4. This indicates that, although wind speed may influence the measurement, it does so by raising the error by a few Celsius degrees. In any case, although the influence of wind has been found to have little impact on the measurement, the ultimate goal of these tests is to lay the groundwork for measuring glass temperature and consequent vacuum partial pressure with a drone in commercial PTC solar fields' environments for corrective prediction of the solar field behaviour. These drone measurements should be made when the wind speed is not very high because strong gusts will make stability and navigation difficult. The differences between environment and glass temperatures produce energetic loss and variation of the glass temperature. In the laboratory there is lower loss and this can be the cause the glass temperature is higher than the measured outdoor. This energetic loss can be obtained using the equation of Stefan Boltzmann, but it is into account of the sky temperature to correct the final glass temperature measured with the IR camera.

It has been visually inspected graphically, on the basis of the Fig. 5, which variables influence the measurement error, reaching the conclusion that wind speed is the most influential variable, as its trend line has the same behaviour as the trend line of the error. It is possible that the wind moves the structure where the IR camera is located in the test campaigns causing variation in the measured temperature. This factor could have affected de measurements realised, but this problem would be avoided when measurements are made with the infrared camera installed on a drone. A covariance and correlation matrix has also been calculated to study numerically which variables are more or less correlated with the mean error. These calculations have been done in Matlab.

Of the covariance and correlation matrices of the Table 1, it can be observed that the correlation of the temperature error is positive with DNI, wind speed, atmospheric pressure and relative humidity, while it has a negative correlation with ambient temperature and wind direction. These positive and negative dependencies between variables are interpretable, for example, the higher the DNI, the more error can be made as solar irradiance can introduce variations in the measurement due to its direct influence on the camera detector. Wind speed also increases the measurement error as its own value increases, as has been observed in the Fig. 5. On the other hand, although relative humidity can affect the measurement error, in the tests recorded during the six months test-campaign very low humidity have been recorded in all the tests, therefore, it is not possible to have conclusive data due to the climate characteristics of the PSA site, it could only be concluded that relative humidity does not affect the infrared measurement at the PSA site. Even so, the correlations of each variable with the error is low, it has been concluded that some affect more because their correlation value is higher, but even so, all of them present a value lower than 0.5.

According to the coefficient matrix, the variables that are least correlated with the error are wind direction, atmospheric pressure and relative humidity. Therefore, it can be considered that they do not affect the IR temperature measurement. The strongest correlated variables with the temperature error are wind speed, DNI and ambient temperature, as they are the variables with the highest coefficient values. The effects of DNI and ambient temperature can be compensated in the measurement process using the Sky temperature obtained with the reflector method, as indicated above.

4.2. Influence of IR camera-source distance on measurement

Fig. 6 shows the results of the tests in the tubes laboratory, showing the glass temperature values for the four different heights and for different temperatures of the receiver tube from the preliminary tests.

It is observed that at a distance 70 cm height there is a difference in the measurement between 3 °C and 5 °C for all the receiver tube temperatures tested.

These differences in the temperature recorded at different heights may be due to the chosen measurement area, i.e. to the AOI (Area of Interest). The projection of each pixel of the area of interest in the camera decreases with height, making the average value of the area

Table 1
Covariance and Correlation Matrix of meteorological variables and measurement error between IR camera outdoors-laboratory measurements. Where Error is the one of the outdoor glass envelope temperature measured with the IR camera compared to the measurements obtained in the laboratory, RH is the Relative Humidity, W10 is the wind speed at 10 m, W12 is the wind speed at 12 m, P is the atmospheric pressure, Wdir is the wind speed direction, DNI is the Direct Normal Irradiance and T is the ambient temperature.

Covariance Matrix

	Error (%)	*T (°C)*	*DNI (W/m2)*	*W12 (m/s)*	*Wdir (°)*	*P (mbar)*	*W10 (m/s)*	*RH (%)*
Error (%)	54,38	−20,54	292,54	9,97	−132,51	11,75	12,12	2,71
T (°C)	−20,54	37,24	−201,87	7,79	−111,57	−22,63	16,14	0,71
DNI (W/m^2)	292,54	−201,9	29021,14	24,37	−867,81	406,44	−132,11	55,79
W12 (m/s)	9,97	7,79	24,37	27,45	−88,15	−20,34	35,22	−10,42
Wdir (°)	−132,51	−111,6	−867,81	−88,15	5131,70	−77,85	−121,18	−138,3
P (mbar)	11,75	−22,63	406,44	−20,34	−77,85	73,63	−33,82	0,28
W10 (m/s)	12,12	16,14	−132,11	35,22	−121,18	−33,82	50,57	−13,87
RH (%)	2,71	0,71	55,79	−10,42	−138,27	0,28	−13,87	63,56

Correlation Matrix

	Error (%)	*T (°C)*	*DNI (W/m2)*	*W12 (m/s)*	*Wdir (°)*	*P (mbar)*	*W10 (m/s)*	*RH (%)*
Error (%)	1,00	−0,46	0,23	0,26	−0,25	0,19	0,23	0,05
T (°C)	−0,46	1,00	−0,19	0,24	−0,26	−0,43	0,37	0,01
DNI (W/m^2)	0,23	−0,19	1,00	0,03	−0,07	0,28	−0,11	0,04
W12 (m/s)	0,26	0,24	0,03	1,00	−0,23	−0,45	0,93	−0,25
Wdir (°)	−0,25	−0,26	−0,07	−0,23	1,00	−0,13	−0,24	−0,24
P (mbar)	0,19	−0,43	0,28	−0,45	−0,13	1,00	−0,56	0,00
W10 (m/s)	0,23	0,37	−0,11	0,93	−0,24	−0,56	1,00	−0,24
RH (%)	0,05	0,01	0,04	−0,25	−0,24	0,00	−0,24	1,00

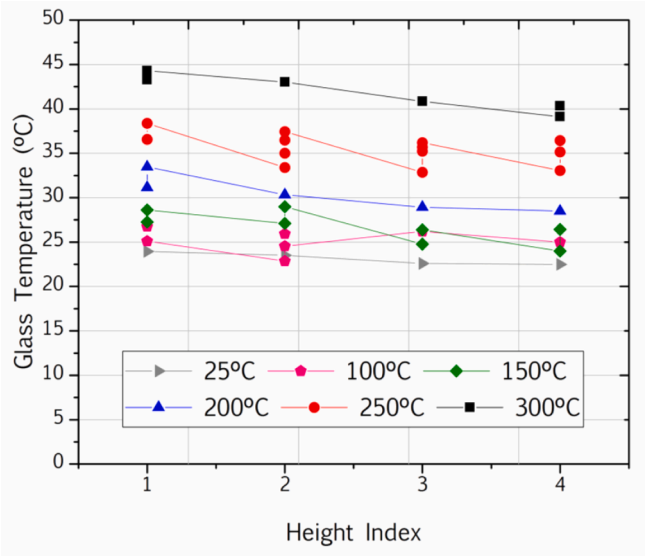

Fig. 6. Glass envelope temperature at different heights and different collector tube temperatures in the laboratory (Height 1 = 118 cm; Height 2 = 124.5 cm; Height 3 = 176.5 cm; Height 4 = 184.5 cm).

smaller, therefore, the value of the recorded temperature decreases. This phenomenon can be seen in the Fig. 7.

It can be seen that the two solid angles ($d\Omega_{scene}$, $d\Omega_{image}$) of the double cone generated from the surface portion of the scene (dA_{scene}) and the image (dA_{image}) to the centre of the lens will be equal. Each of the solid angles, under which the scene and the image are viewed from a point at the centre of the lens, is calculated as the projection of the object onto a sphere of radius equal to the distance from the centre of the lens to the object (l_{scene}) and to the image (l_{image}), the solid angle is the projection of the object onto the sphere, divided by the distance from the centre to the scene, being the same for the image.

$$d\Omega_{image} = d\Omega_{scene} \tag{6}$$

$$\frac{dA_{image}\cos(\theta)}{\left(\frac{l_{image}}{\cos(\theta)}\right)^2} = \frac{dA_{scene}\cos(\varpi)}{\left(\frac{l_{scene}}{\cos(\theta)}\right)^2} \tag{7}$$

$$\frac{dA_{scene}}{dA_{image}} = \frac{\cos(\theta)}{\cos(\varpi)}\left(\frac{l_{scene}}{l_{image}}\right)^2 \tag{8}$$

Continuing with Fig. 7, the solid angle subtended by the lens would be defined in the same way by means of the Eq. (9), where the area of the lens would be the area of a circle.

$$d\Omega_{lent} = \frac{lens\,Area}{(distance_{lens-scene})^2} \tag{9}$$

$$d\Omega_{lens} = \frac{\pi d^2\cos(\theta)}{4\left(\frac{l_{scene}}{\cos(\theta)}\right)^2} \tag{10}$$

The radiation flux received at the lens (radiance, q) from the surface portion dA_{scene}, is the same as the projected radiation flux (irradiance, I) at the image portion dA_{image}.

$$q(dA_{scene}\cos(\varpi))d\Omega_{lens} = IdA_{image} \tag{11}$$

Eqs. (8), (10) and (11) give Eq. (12), where it can be seen that the irradiance of the image is proportional to the radiance of the scene. Furthermore, the field of view is very small, so the effect of the cosine to the fourth is very small, almost negligible in the equation, as ϖ and θ are very small angles. Thus, the integrated radiant flux in the pixel, ϕ, will be expressed by Eq. (13).

$$I = q\frac{\pi}{4}\left(\frac{d^2}{l_{image}}\right)^2\cos^4(\theta) \tag{12}$$

$$\Phi = \frac{dA_{scene}\pi d^2}{dA_{image}4l_{scene}^2}t_{int}\int_0^\infty q(\lambda)S(\lambda)\tau_{s.o.}(\lambda)d\lambda \tag{13}$$

Where S(λ) is the spectral response of the pixel, t_{int} is the integration or exposure time of the camera and $\tau_{s.o.}$ is the transmittance of the optical system [16,17,18].

In order to determine an empirical correlation between the distance and the decrease in the temperature reading measured in the camera, due to the observed importance of this phenomenon, further tests were carried out in addition to those in the laboratory, varying the camera-tube distance to more realistic ones according to the drone-tube distances that would be present in the real operation of a plant, with the experimental device shown in the Fig. 2 (b). These tests have been carried out at 1 m, 2 m, 3 m, 4 m and 5 m distance. For this purpose, in this case, a minimum pixel size of the AOI to be measured has been chosen in order to study whether this minimises the effect of the temperature variation measured with the IR camera-source distance, as detailed according to the phenomenon of the Fig. 7.

Fig. 8 shows that after measuring the temperature using an AOI of the smallest possible pixel size, there are no significant differences in the glass envelope temperature recorded at different distances, except for the 400 °C absorber tube temperature. The deviation of each of the temperatures at different heights from the average glass envelope temperature at each absorber temperature is 1.65 °C for 100 °C, 1.74 °C for 200 °C, 0.80 °C for 300 °C and 3.45 °C for 400 °C. It can be seen that the differences are less than 2 °C in all cases except for 400 °C, which may be due to the intrinsic error of the measurement itself, rather than to the

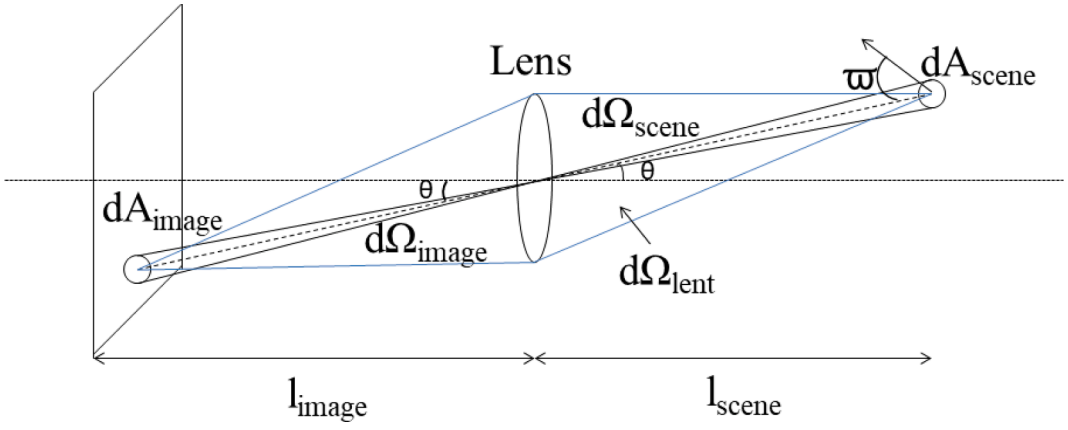

Fig. 7. Diagram of convergent lens optics.

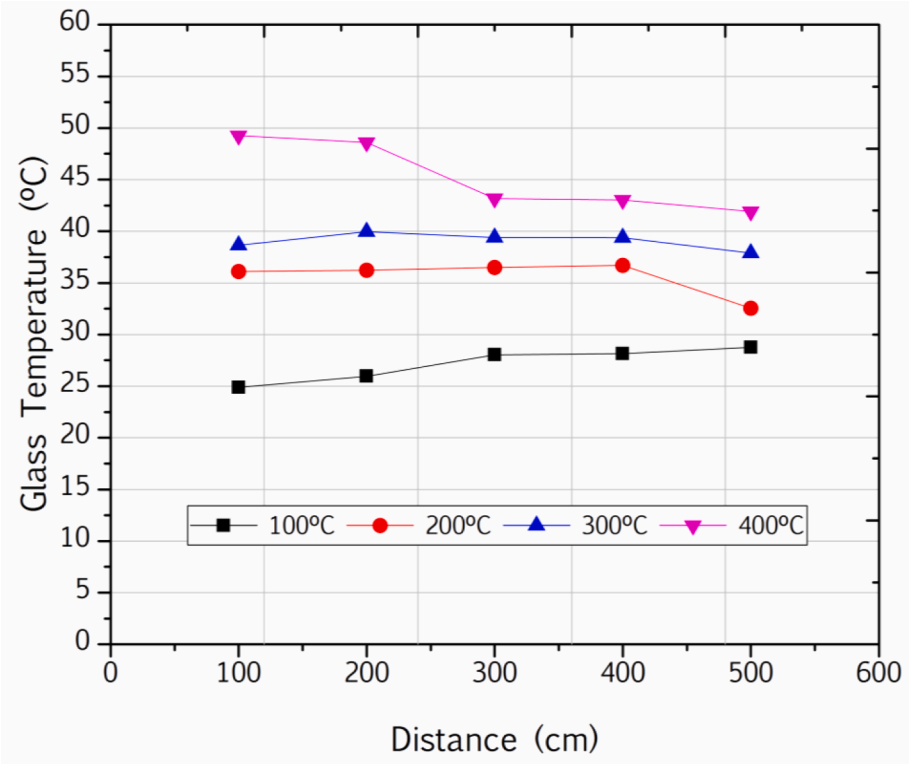

Fig. 8. Glass envelope temperature for different absorber tube temperatures at distances between the IR camera and receiver tube of 100 cm, 200 cm, 300 cm, 400 cm and 500 cm.

variation of the source-IR camera distance.

In the case of measurement with digital cameras this problem has been solved by using lenses with a specific focal length to make the projection matrix of the measurement-pixel area the same with distance [18]. In the case of infrared cameras, it is more difficult to use magnifying lens because their spectral transmittance does not cover the

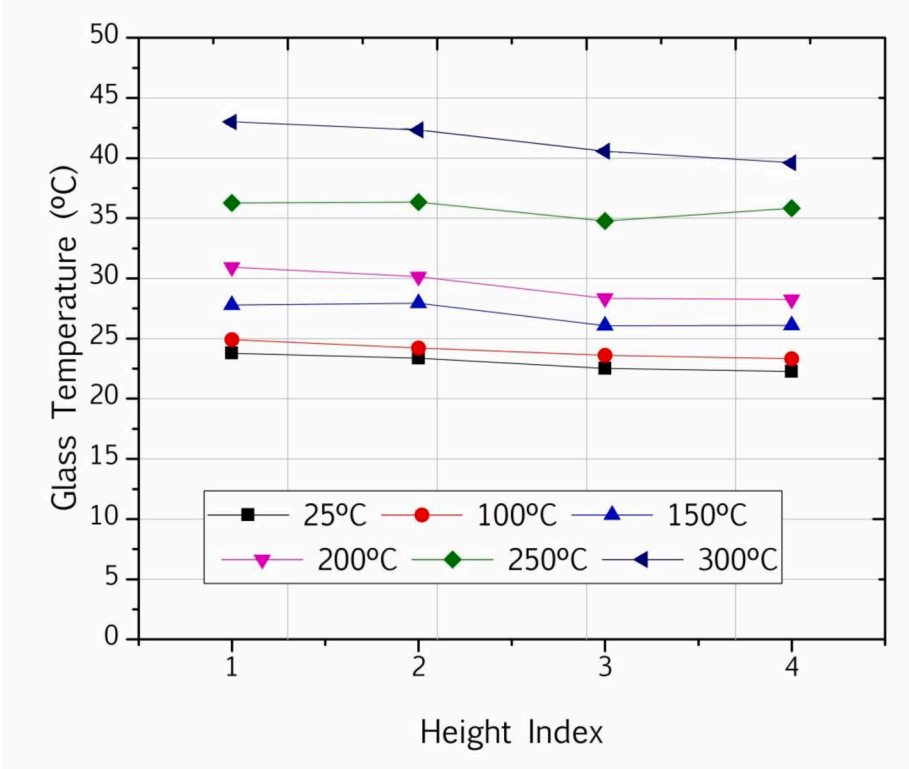

Fig. 9. Glass envelope temperature at different heights and different collector tube temperatures carried out in the laboratory by choosing a smaller AOI (Height 1 = 118 cm; Height 2 = 124.5 cm; Height 3 = 176.5 cm; Height 4 = 184.5 cm).

spectral value of the camera. Therefore, selecting an AOI or measurement area with the smallest possible pixel size minimises the variation of the temperature measurement with height, both in outdoor and laboratory measurements. In the latter, to see the difference, choose an AOI of the smallest possible pixel size to measure, as shown in the Fig. 9.

In Fig. 9 a smaller AOI of the smallest possible number of pixels has been chosen, using a measure point of 1x1 pixels of dimensions, and it has been found that the temperature difference due to height improves significantly; the variation is only a few degrees Celsius, and it may be due to the intrinsic uncertainties of the measurement process.

Other authors correct this problem by using the concept of Source Size Effect (SSE) [19]. SSE is the result of various optical phenomena such as diffraction, aberrations, refraction and scattering of the radiation in the measuring instrument. These phenomena blur the radiometric image and cause shadowing of the field of view boundary. In addition, scattering causes the detector element to miss the radiation in the FOV and to detect radiation outside the FOV, making the infrared image composed of pixels arranged in rows and columns, representing an element of the detector, smaller. The result is that the radiation received by the detector depends on the size and environment of the measured object. Several solutions can be found when calibrating to correct this effect [20]. Special lenses and minimisation of optical imperfections can reduce the amount of SSE [21]. In the work by Kruse et al. [19], a blackbody calibration is used to identify the SSE, on the basis that the crucial parameter for the SSE identification is the angular target size of the blackbody calibration source. For the calibration, various angular target sizes are set by varying the distance from the IR camera to the blackbody. The angular target size of the initial factory calibration is found when the temperature measured by the IR camera matches the blackbody temperature. The correct radiometric signal without influence of the SSE will be measured for an angular target size of 180°. Thus, the SSE factor is calculated by relating the measured value to a reference value, then, since the error of the IR cameras is minimised in the factory calibration, the respective signal value is chosen as reference.

4.3. Comparison between the Sky Temperature obtained with a reflector or through the mirror of the parabolic trough collector itself

During the outdoor tests to obtain the influence of meteorological variables on the average temperature of the glass envelope, the Sky temperature necessary to obtain the final temperature measurement was obtained using the Surface Temperature Method, by adding a reflector to the experimental device and obtaining it from the reflector of the PTC itself. In the IR camera measurements of these two reflectors, an emissivity of 1 was used for them, considering that all the radiation was emitted. The data from both reflectors have been compared to estimate whether in real field measurements with a drone, this Sky temperature can be measured directly from the solar collector's reflector instead of using a mirror facet sample as in the case of the solar field tests. Fig. 10 shows the difference in the Sky temperature recorded in each test between the mirror sample temperature and the mirror facet. It can be seen that there is a systematic difference between the Sky temperature values using each of the two mirrors, although the value in both cases follows the same trend line. In Fig. 11 a comparison of both Sky temperatures has been made and it can be seen, that according to Pearson's coefficient R = 0.96, both temperatures do not differ significantly from each other. The trend line has been marked in a linear regression and it can be seen that both temperatures are coincident with a difference of 8 °C in both cases. If we apply the correction of these 8 °C to the Sky temperature of the mirror facet, it will be the same as the reference temperature as the Sky temperature of the sample mirror. The correction would be given by the Eq. (14) where T_{facet} is the Sky temperature of the mirror facet and $T_{mirror\ sample}$ is the Sky temperature of the sample mirror.

$$T_{facet} = 8.13 + 0.90 T_{mirrorsample} \quad (14).$$

This difference in temperature between the two mirrors may be due to two reasons. On the one hand, because emissivity 1 has been considered in both mirrors. Actually the value 1 would be for the

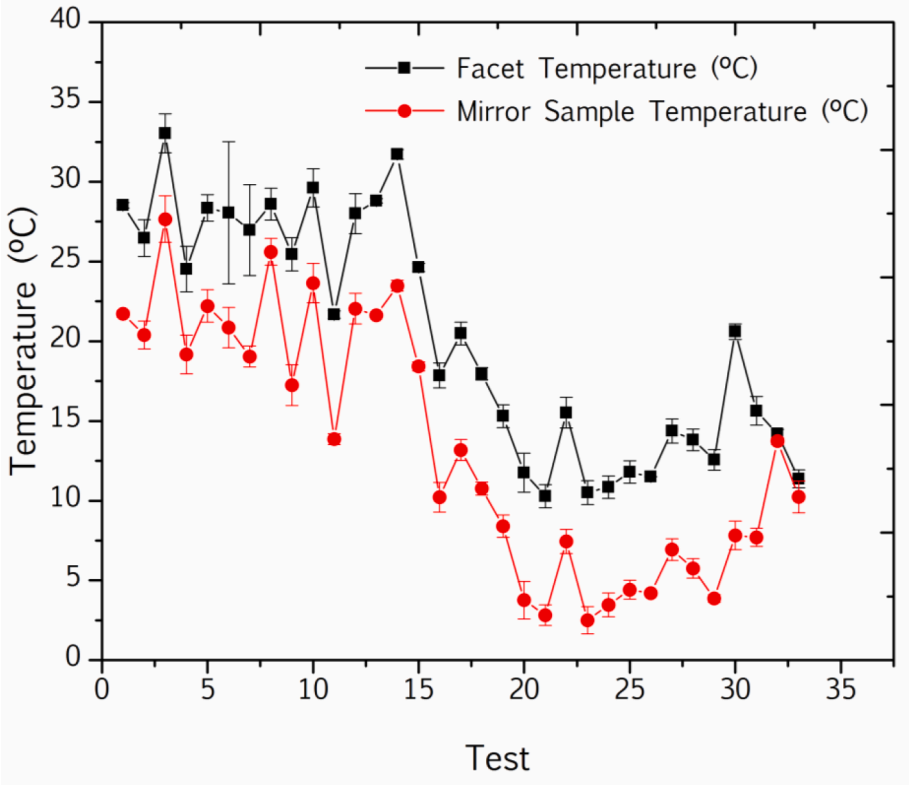

Fig. 10. Sky Temperature recorded at each test using the sample mirror and the mirror facet.

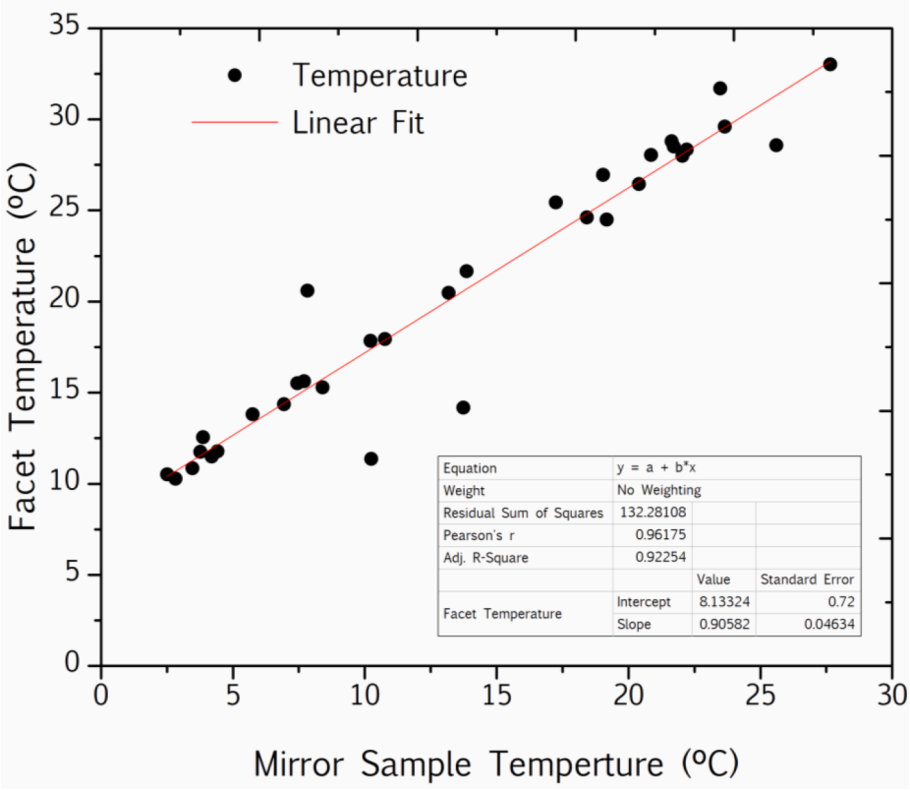

Fig. 11. Comparison of the mirror sample and the mirror facet temperature.

reflectivity, but it is common practice in infrared thermography to consider the emissivity of the reflector to be 1 in order to take into account in the calculations all the emitted radiation (actually the reflected radiation, since the mirror would not have high temperature to emit much thermal radiation. It has been assumed that, being a perfect reflector (reflectance equals 1), it can be considered that everything reflected has been emitted and therefore emissivity 1 is assumed. If we then consider instead of emissivity 1 for the facet, emissivity 0.9–0.95, the measured Sky temperature would be of the order of 2 or 3°lower, resembling even more the Sky temperature measured using the mirror sample temperature. In addition, as can be seen in the Fig. 1, in the outdoor test setup, the distance between the IR camera and the sample temperature mirror is smaller than the distance between the IR camera and the mirror facet, therefore the measurement error is made due to the sensor-source distance as mentioned in the previous sections. It also can be possible that the temperature of both mirror are different showing distinct thermographic measurements. Therefore, taking into account these aspects that introduce difference in the measurement using the two different mirrors, and taking into account the data of Fig. 10 and Fig. 11, where it can be seen that there is only a systematic difference of about 8 °C in all measurements, it can be considered feasible to use the Sky temperature measured directly from the mirror facet in parabolic trough solar fields, taking into account the correction of the infrared sensor-camera distance.

4.4. Conclusion

The influence of meteorological variables on the measurement of vacuum partial pressure with IR camera temperature measurement using the Surface Temperature method has been analysed, observing that wind speed is the variable that has the greatest effect, although the wind speed recorded at the location where the tests were carried out was not extremely high. The influence of the sensor-source distance on the infrared thermography has also been studied comparing laboratory and outdoor tests, reaching the conclusion that by taking a smaller AOI the differences are reduced. Finally, it has been verified that for measurements in a PTC solar field, it is possible to obtain the Sky temperature value required for infrared measurements directly from the reflector of the solar collector itself, using a small AOI. Thanks to the new point of view of the method, it is possible to determine the partial vacuum losses in PTC with methods that do not interfere with the operation, since it was necessary to determine if the proposed method works to carry out measurements with drones in commercial plants.

Declaration of Competing Interest

The authors declare that they have no known competing financial interests or personal relationships that could have appeared to influence the work reported in this paper.

Data availability

Data will be made available on request.

Acknowledgments

We gratefully acknowledge the financial support by the European Union's Horizon 2020 research and innovation programme (Project SFERA-III – Grant Nr. 823802).

References

[1] G. Espinosa-Rueda, J. Hermoso, N. Martínez-Sanz, M. Gallas-Torreira, Vacuum evaluation of parabolic trough receiver tubes in a 50 MW concentrated solar power plant, Sol. Energy 139 (2016) 36–46.
[2] S. Dreyer, P. Eichel, T. Gnaedig, Z. Hacker, S. Janker, T. Kuckelkorn, et al., Heat Loss Measurements on Parabolic Trough Receivers, in: Proceedings of the SolarPACES Conference 2010. Perpignan (France), 2010.

[3] J. Wang, X. Huang, G. Gong, M. Hao, F. Yin, A systematic study of the residual gas effect on vacuum solar receiver, Energy Convers. Manage. 52 (6) (2011) 2367–2372.
[4] C. Simon, M. Röger, Modelling, Simulation and Identification of Heat Loss Mechanisms for Parabolic Trough Receivers Installed in Concentrated Solar Power Plants, IFAC-PapersOnLine 48 (1) (2015) 372–377.
[5] M. Röger, P. Potzel, J. Pernpeintner, S. Caron, A Transient Thermography Method to Separate Heat Loss Mechanisms in Parabolic Trough Receivers, J. Sol. Energy Eng. 136 (011006) (2014) 1–9.
[6] M. Yaghoubi, F. Ahmadi, M. Bandehee, Analysis of heat transfer losses of absorber tubes of parabolic trough collector of Shiraz (Iran) solar power plant, J. Clean Energy Technol. 1 (1) (2013) 33–37.
[7] X. Olano, A. de Jalón, D. Pérez, J. Barberena, J. López, M. Gastón, Outcomes and features of the inspection of receiver tubes (ITR) system for improved O&M in parabolic trough plants, in: AIP Conference Proceeding, vol. 2033, 2018.
[8] M. Pfänder, E. Lüpfert, P. Pistor, Infrared temperature measurements on solar trough absorber tubes, Sol. Energy 81 (5) (2007) 629–635.
[9] E. Setien, R. López-Martín, L. Valenzuela, Methodology for partial vacuum pressure and heat losses analysis of parabolic troughs receivers by infrared radiometry, Infrared Phys. Technol. 98 (2019) 341–353.
[10] G.B. Dalton, M. Caldwell, A.K. Ward, M.S. Whalley, G. Woodhouse, R.L. Edeson, … J.P. Emerson, The VISTA infrared camera, in: Paper presented at the Proceedings of SPIE - the International Society for Optical Engineering, 6269, 2006.
[11] E. Lüpfert, M. Geyer, W. Schiel, A. Esteban, R. Osuna, E. Zarza, P. Nava, Eurotrough design issues and prototype testing at PSA, in: Paper presented at the International Solar Energy Conference, 2001, 387–391. doi: 10.1115/sed2001-149.
[12] F. Sutter, S. Meyen, A. Fernández-García, P. Heller, Spectral characterization of specular reflectance of solar mirrors, Sol. Energy Mater. Sol. Cells 145 (2016) 248–254.
[13] ASTM E2847-14, 2015. Standard Test method for Calibration and Accuracy Verification of Wideband Infrared Thermometers, ASTM Int. West Conshohocken, West Conshohocken.
[14] F. Sallaberry, L. Valenzuela, L.G. Palacin, ON-site parabolic-trough collector testing in solar thermal power plants: Experimental validation of a new approach developed for the IEC 62862-3-2 standard, Solar Energy 155 (2017) 398–409.
[15] F. Sakuma, S. Hattori, Establishing a practical temperature standard by using a narrow-band radiation thermometer with a silicon detector. Measurement and Control in Science and Industry. New York: Schooley, J.F, 1982, 421-427.
[16] J. Ballestrín, E. Carra, J. Alonso-Montesinos, G. López, J. Polo, A. Marzo, et al., Modeling solar extinction using artificial neural networks. Application to solar tower plants. Energy 199 (2020).
[17] J. Alonso-Montesinos, R. Monterreal, J. Fernández-Reche, J. Ballestrín, E. Carra, J. Polo, et al., (s.f.). Intra-hour energy potential forecasting in a central solar power plant receiver combining meteosat images and atmospheric extinction, Energy 188.
[18] J. Ballestrín, E. Carra, R. Monterreal, R. Enrique, J. Polo, J. Fernández-Reche, et al., One year of solar extinction measurements at plataforma solar de almería. Application to solar tower plants. Renew. Energy 136 (2019) 1002-1011.
[19] L. Kruse, S. Caron, Analysis of temperature measurements on solar absorber coatings under concentrated solar flux. Paderborn: Master Thesis, 2019.
[20] T. Ricoli, L. Wang, Experiments and remarks on the size source effect in precision radiation thermometry. 93, 1993.
[21] M. Ohtsuka, R.E. Bedford, Measurement of size source effects in an optical pyrometer, Measurement 1 (7) (1989) 2–6.